

## Coupling Diffuse Sky Radiation and Surface Albedo

BERNARD PINTY,<sup>\*</sup> ALESSIO LATTANZIO,<sup>+</sup> JOHN V. MARTONCHIK,<sup>#</sup> MICHEL M. VERSTRAETE,<sup>\*</sup>  
NADINE GOBRON,<sup>\*</sup> MALCOLM TABERNER,<sup>\*</sup> JEAN-LUC WIDLowski,<sup>\*</sup> ROBERT E. DICKINSON,<sup>@</sup> AND  
YVES GOVAERTS<sup>&</sup>

<sup>\*</sup>Global Vegetation Monitoring Unit, IES, EC Joint Research Centre, Ispra, Italy

<sup>+</sup>Makalumedia gmbh, Darmstadt, Germany

<sup>#</sup>Jet Propulsion Laboratory, California Institute of Technology, Pasadena, California

<sup>@</sup>School of Earth and Atmospheric Sciences, Georgia Institute of Technology, Atlanta, Georgia

<sup>&</sup>EUMETSAT, Am Kavalleriesand, Darmstadt, Germany

(Manuscript received 29 July 2004, in final form 3 November 2004)

### ABSTRACT

New satellite instruments have been delivering a wealth of information regarding land surface albedo. This basic quantity describes what fraction of solar radiation is reflected from the earth's surface. However, its concept and measurements have some ambiguity resulting from its dependence on the incidence angles of both the direct and diffuse solar radiation. At any time of day, a surface receives direct radiation in the direction of the sun, and diffuse radiation from the various other directions in which it may have been scattered by air molecules, aerosols, and cloud droplets. This contribution proposes a complete description of the distribution of incident radiation with angles, and the implications in terms of surface albedo are given in a mathematical form, which is suitable for climate models that require evaluating surface albedo many times. The different definitions of observed albedos are explained in terms of the coupling between surface and atmospheric scattering properties. The analytical development in this paper relates the various quantities that are retrieved from orbiting platforms to what is needed by an atmospheric model. It provides a physically simple and practical approach to evaluation of land surface albedo values at any condition of sun illumination irrespective of the current range of surface anisotropic conditions and atmospheric aerosol load. The numerical differences between the various definitions of albedo for a set of typical atmospheric and surface scattering conditions are illustrated through numerical computation.

### 1. Introduction

Albedo at some level  $z$  of a geophysical system is defined as the ratio between the upward flux density or irradiance exiting that particular level and the downward flux density impinging on that same level  $z$ . This quantity is needed for many purposes including an assessment of the partitioning between the radiant fluxes absorbed by the atmosphere and the surface. It can be estimated at any wavelength and over any spectrally integrated region of the spectrum. Its dependency on the vertical coordinate  $z$  complicates such estimates when the medium located above that level  $z$  is able to interact and thus to modify both the intensity and the

angular distribution of the field of downwelling intensities originally available at the top of the atmosphere. This situation occurs when estimating the albedo of a land surface intercepting solar radiation at level  $z_0$  after it has traveled through the entire column of an absorbing and scattering atmosphere: the surface albedo, so defined as a radiant flux ratio, is not an intrinsic property of the surface but rather determined by both the surface and the overlying atmospheric layers.

A proper estimation of land surface albedo requires, therefore, consideration of the absorbing and scattering properties of the atmosphere that are controlling the field of downwelling intensities at level  $z_0$ . This modification of the radiation depends on minor constituents (i.e., water vapor, carbon dioxide, ozone and other pollutants, clouds, and aerosols), whose concentrations may be highly variable in space and time, or with poorly constrained optical properties (e.g., gaseous and particulate emissions from industrial, agricultural and

---

Corresponding author address: B. Pinty, Global Vegetation Monitoring Unit, IES, EC Joint Research Centre, TP 440, via E. Fermi, I-21020 Ispra (VA), Italy.  
E-mail: bernard.pinty@jrc.it

transportation activities, biomass burning, and dust). Consequently, the field of downward radiation at the bottom of the atmosphere ( $z_0$ ) is spatially heterogeneous, temporally dynamic, and spectrally and angularly dependent. The difficulty of accurately estimating the upward flux density at the bottom of the atmosphere ( $z_0$ ) is further compounded by the fact that all land surfaces themselves exhibit substantial spectral and anisotropic properties: they absorb and scatter solar radiation differently in different directions, and they do so differently at different wavelengths. These complex processes depend not only on the nature and optical properties of the objects that constitute the surface, but also on their structure and spatial heterogeneity. The interaction between the downward irradiance reaching the bottom of the atmosphere at level  $z_0$  and the surface is thus complicated and its representation through a single number, often called albedo, can mask this complexity.

Space-based measurements now document the state and evolution of the global land surface under cloud-free conditions, as well as characterize properties of the atmosphere. Regional and global surface albedo products are thus becoming available that are useful for better representing land surface processes, such as in climate models. All such products are based on ratios between upward and downward radiant fluxes. They make various assumptions as to how atmospheric scattering processes determine the downward diffuse intensities. If the atmospheric scattering effects are removed, the measured radiant fluxes become datasets of directional hemispherical reflectance (DHR), a quantity that is an intrinsic surface property. If the atmospheric scattering contributions are included, the resulting datasets are the bihemispherical reflectances (BHR). These depend on the ambient atmospheric and sun zenith angle conditions (see, e.g., Martonchik et al. 2000). If all the radiation reaching the surface can be assumed to be isotropic, retrieval algorithms deliver a  $BHR_{iso}$  value corresponding to a flux ratio that is, again, independent of ambient conditions. For instance, the National Aeronautics and Space Administration (NASA) Moderate Resolution Imaging Spectroradiometer (MODIS) sensor on *Terra* delivers DHRs and  $BHR_{iso}$  [these products are called black sky and white sky albedos, respectively; Schaaf et al. (2002)], while the retrieval algorithm selected for the processing of data acquired by the NASA Multiangle Imaging Spectroradiometer (MISR) sensor on *Terra* generates DHRs, as well as BHRs but for the particular sun illumination conditions at the time of the satellite measurement only (Martonchik et al. 1998b). Based on the algorithm proposed by Pinty et al. (2000a) to analyze Meteosat measurements,

the European Organisation for the Exploitation of Meteorological Satellites (EUMETSAT) delivers surface albedo product corresponding to DHRs for a fixed sun zenith angle.

These products are, in fact, complementary since they do not represent the same physical quantities and the selection of one particular product in this panoply is thus driven by the application at hand. They provide means to better represent land surface processes in general, and land surface albedo in particular, in atmospheric general circulation models (see, e.g., Zhou et al. 2003; Knorr et al. 2001; Roesch et al. 2004). The lower atmospheric boundary conditions are increasingly recognized as of importance for weather prediction and even more so for longer climatic time scales. As the duration of the time integration increases (multiple days and beyond), the relative importance of surface processes becomes progressively more critical because of their cumulative effects on the overall energetics of the atmosphere (see, e.g., Verstraete 1989).

Surface albedo products derived from remote sensing are currently being used to improve the accuracy of the simulations of global climate models provided they can prescribe or generate physical quantities equivalent to those currently delivered by space agencies. To do so requires that the models include the coupling between the atmosphere and the surface scattering processes needed to represent accurately the ratios of upward to downward radiant fluxes, that is, the BHRs 1) for any given solar position, that is, for any grid cell in the model at any time of the day or season, and 2) for any arbitrary state and composition of the overlying atmosphere, that is, for any particular irradiance field that may result from the distribution of clouds and aerosols computed by the atmospheric model.

This paper discusses the scientific issues associated with the coupling between the atmospheric and surface layers, evaluates the differences between the various albedo products, and helps bridge the gap between the remote sensing and the climate simulation communities. Specifically, it investigates the analytical relationships that exist between the DHRs, the BHRs, and the  $BHR_{iso}$  and then evaluates the differences between these products based on a series of radiation transfer simulations. It proposes an analytical, highly accurate procedure to couple land surfaces with the overlying atmospheric models for a wide range of sun zenith angle values and aerosol load conditions.

## 2. From downward to upward intensity fields

The total downwelling spectral intensity or radiance in units of  $W m^{-2} sr^{-1} \mu m$  reaching the surface,

$I^{\downarrow\text{tot}}(z_0, \mathbf{\Omega}_0, \mathbf{\Omega}; \tau, \rho_{\text{sfc}})$  through a plane-parallel atmosphere can be written as a sum of multiple contributions depending on the nature and relative importance of the scattering processes that are involved as well as on our current capability to estimate these contributions using efficient computer techniques. For most atmospheric global/regional models applications, the decomposition of the total downwelling spectral intensity field into the following three contributions should be appropriate [see, e.g., Liou (1980), chapter 6]:

$$\begin{aligned} I^{\downarrow\text{tot}}(z_0, \mathbf{\Omega}_0, \mathbf{\Omega}; \tau, \rho_{\text{sfc}}) &= I^{\downarrow\text{dir}}(z_0, \mathbf{\Omega}_0, \mathbf{\Omega}; \tau) \\ &+ I_B^{\downarrow\text{diff}}(z_0, \mathbf{\Omega}_0, \mathbf{\Omega}; \tau) \\ &+ I_{\text{ms}}^{\downarrow\text{diff}}(z_0, \mathbf{\Omega}_0, \mathbf{\Omega}; \tau, \rho_{\text{sfc}}), \end{aligned} \quad (1)$$

where  $I^{\downarrow\text{dir}}$  corresponds to the intensity directly transmitted to the surface at level  $z_0$  along the direction  $\mathbf{\Omega}_0(\mu_0, \phi_0)$ ,  $I_B^{\downarrow\text{diff}}$  expresses the downwelling intensity due to multiple scattering into the atmosphere only that is overlying a hypothetical black surface and is thus diffusely transmitted to the surface in direction  $\mathbf{\Omega}(\mu, \phi)$ , when the sun is located in direction  $\mathbf{\Omega}_0(\mu_0, \phi_0)$ . Here,  $I_{\text{ms}}^{\downarrow\text{diff}}$  represents the additional downwelling intensity induced by the radiation that undergoes multiple interactions between the actual surface and the atmosphere. This latter term thus logically depends on the surface scattering properties that are specified using the surface bidirectional reflectance factor (BRF),  $\rho_{\text{sfc}}$  [see Nicodemus et al. (1977) and Martonchik et al. (2000) for definitions]. All three contributions listed in (1) obviously depend on the absorbing and scattering properties of the atmosphere as well as its optical depth and, unless stated otherwise, are deemed monochromatic quantities. Any direction  $\mathbf{\Omega}$  is characterized by a zenith angle whose cosine is equal to  $\mu$  and an azimuth angle noted  $\phi$  (the subscript 0 identifies the particular direction of the sun). In these equations, the first (second) argument after  $z_0$  indicates the direction of incident (transmitted or scattered) intensity, and the plus/downward (minus/upward) signs specify the downward (upward) direction as appropriate.

These intensities are the basic quantities required to estimate the associated downward flux densities or irradiances needed for modeling land surface processes. For practical purposes, it is often convenient to express these intensities using normalized (scattering and transmission) functions that are independent of the external downward source of radiation, namely the sun. One can thus formulate the intensities reaching the surface level through bidirectional transmission distribution functions in units of  $\text{sr}^{-1} \mu\text{m}$ , in order to make explicit the

dependencies with respect to the direction of interest,  $\mathbf{\Omega}(\mu, \phi)$ , and the direction of the main external source,  $\mathbf{\Omega}_0(\mu_0, \phi_0)$ . Such an approach yields the following set of equations for the direct and diffuse bidirectional transmission functions, respectively:

$$\begin{aligned} \exp(-\tau/\mu_0) &= I^{\downarrow\text{dir}}(z_0, \mu_0, \mu, \phi_0 \\ &- \phi; \tau)/E_0 \delta(\mu_0 - \mu) \delta(\phi_0 \\ &- \phi), \end{aligned} \quad (2)$$

$$\begin{aligned} T_B(z_0, \mu_0, \mu, \phi_0 - \phi; \tau) &= I_B^{\downarrow\text{diff}}(z_0, \mu_0, \mu, \phi_0 \\ &- \phi; \tau)/E_0 \mu_0, \end{aligned} \quad (3)$$

and

$$\begin{aligned} T_{\text{ms}}(z_0, \mu_0, \mu, \phi_0 - \phi; \tau, \rho_{\text{sfc}}) &= I_{\text{ms}}^{\downarrow\text{diff}}(z_0, \mu_0, \mu, \phi_0 \\ &- \phi; \tau, \rho_{\text{sfc}})/E_0 \mu_0, \end{aligned} \quad (4)$$

where  $E_0$  is the collimated spectral extraterrestrial solar irradiance, that is, the solar flux density normal to the incident beam in units of  $\text{W m}^{-2} \mu\text{m}$ ,  $\delta$  is the Dirac's delta function, and  $\tau$  is the vertical atmospheric optical depth. Since the atmosphere is composed of infinitely small and nonoriented elements, the diffuse intensities can be expressed as a function of the relative azimuth angle,  $\phi_0 - \phi$ .

While estimating the direct intensity is analytical and straightforward, all other contributions require extensive computer simulations to solve the radiation transfer equation [see, e.g., Lenoble (1985) and Lyapustin (2002)]. For most modeling as well as remote sensing inversion purposes, the contributions expressed through (3) and (4) must be parameterized as a computer efficient but accurate algorithm. The contribution due to (3) depends only on atmospheric properties and is thus much simpler to evaluate than the one due to (4), which involves multiple scattering between the atmosphere and the surface. Until recently, surface reflectances, in the form of surface BRF values, were not available at the global scale and at temporal and spatial resolutions appropriate for atmospheric model applications. Thanks to the data routinely acquired by sensors on board the *Terra* platform, in particular from the MISR (Diner et al. 1998), such information is now accessible over most surface types and atmospheric models can benefit immediately from these unique datasets. The amplitude of the contribution noted  $I_{\text{ms}}^{\downarrow\text{diff}}$  is controlled by both the amplitude of the surface BRF and the backscattering coefficient of the lowest atmospheric layers, while its angular distribution results from a convolution between the angular functions describing the

anisotropy of the atmospheric downward direct plus diffuse intensity and of the surface BRF. Before inspecting further this coupled contribution, we first focus on the downward diffuse intensity field for a black surface condition (3) that involves atmospheric properties only.

The following mathematical developments take advantage of the strategy proposed for the MISR instrument to retrieve the aerosol load over dark surfaces (Martonchik et al. 1998a) and further extended to any surface type to jointly estimate the surface albedo and the aerosol load from geostationary satellite data (Pinty et al. 2000a). This strategy permits us, first, to limit the computational cost associated with the operational estimation of (3) and, second, to decouple the surface and the atmospheric contribution controlling (4). It is assumed that the diffuse bidirectional transmission distribution function for a black surface condition, namely  $T_B$  as defined by (3), can be expanded as a cosine Fourier series with respect to the relative azimuth angle. With the Fourier expansion limited to the first two components, this transmission function is approximated by

$$T_B(z_0, \mu_0, \mu, \phi_0 - \phi; \tau) \approx T_0(\mu_0, \mu; \tau) + T_1(\mu_0, \mu; \tau) \cos(\phi_0 - \phi), \tag{5}$$

where the coefficients noted with an index 0 and 1 represent the first two Fourier components (with omission of the vertical coordinate  $z_0$ ), respectively, that is,

$$T_0(\mu_0, \mu; \tau) = \frac{1}{2\pi} \int_0^{2\pi} T_B(z_0, \mu_0, \mu, \phi_0 - \phi; \tau) d\phi \tag{6}$$

and

$$T_1(\mu_0, \mu; \tau) = \frac{1}{\pi} \int_0^{2\pi} T_B(z_0, \mu_0, \mu, \phi_0 - \phi; \tau) \cos(\phi_0 - \phi) d\phi. \tag{7}$$

The forthcoming developments capitalize extensively on the reciprocal properties of the diffuse bidirectional transmission distribution functions [see, e.g., Chandrasekhar (1960), chapter 7] such that in our case, for instance,

$$T_0(\mu_0, \mu; \tau) = T_0(\mu, \mu_0; \tau) = T_0(-\mu, -\mu_0; \tau). \tag{8}$$

Note that different reciprocity relations than (8) may hold depending on the definition adopted for the diffuse bidirectional transmission distribution functions,

for example, without normalization by  $\mu_0$  of the intensities.

Since the downward flux density (in  $W m^{-2} \mu m$ ) at the surface is estimated from

$$E^{\downarrow tot}(z_0, \mu_0; \tau) = \int_0^{2\pi} \int_0^1 I^{\downarrow tot}(z_0, \mu_0, \mu, \phi_0 - \phi; \tau) \mu d\mu d\phi, \tag{9}$$

then, given (2), the flux directly transmitted to the surface is simply expressed as

$$E^{\downarrow dir}(z_0, \mu_0; \tau) = E_0 \mu_0 \exp(-\tau/\mu_0), \tag{10}$$

and, following (3) and (5), the downward flux diffusively transmitted to the surface without accounting for the multiple scattering processes between the surface and the atmosphere becomes

$$E_B^{\downarrow diff}(z_0, \mu_0; \tau) = E_0 \mu_0 \bar{T}(\mu_0; \tau), \tag{11}$$

with

$$\bar{T}(\mu_0; \tau) = 2\pi \int_0^1 T_0(\mu_0, \mu; \tau) \mu d\mu. \tag{12}$$

Note that, according to (11) and (3),  $\bar{T}(\mu_0)$  corresponds to the directional hemispherical transmission factor associated with the downward flux diffusively transmitted at level  $z_0$  for a black surface condition.

The term  $T_{ms}$  in (4) expresses the additional contribution to be accounted for when the surface is not radiatively black. It is the most complex contribution in this radiation transfer problem as  $T_{ms}$  depends on the joint surface and atmospheric scattered fields, that is, the amplitude and angular field of both the incoming atmospheric intensities and the surface BRF. The latter can be expressed using the parametric Rahman–Pinty–Verstraete (RPV) model (Rahman et al. 1993), which splits a BRF field into a scalar amplitude component,  $\rho_0$ , and an angular function,  $\check{\rho}_{sfc}$  (implementing itself the product of three functions) to describe the anisotropy of the surface

$$\rho_{sfc}(z_0, \mathbf{\Omega}_0, \mathbf{\Omega}; \rho_0, \rho_c, \Theta, k) = \rho_0 \check{\rho}_{sfc}(z_0, \mathbf{\Omega}_0, \mathbf{\Omega}; \rho_c, \Theta, k). \tag{13}$$

The parameter  $k$ , which enters a modified version of the Minnaert’s function (Minnaert 1941), controls the bowl or bell shape of the BRF fields (Pinty et al. 2002), the parameter  $\Theta$  establishes the degree of forward versus backward scattering (Pinty et al. 2003), depending on its sign, following the Henyey–Greenstein formulation (Henyey and Greenstein 1941) and the parameter  $\rho_c$  accounts for the hot spot effect especially significant at or near the backscattering direction. We will neglect this latter contribution in the subsequent develop-

ments. In the case of a Lambertian surface, that is, the upward intensity field is scattered isotropically,  $\check{\rho}_{\text{sfc}}$  becomes constant and equal to unity by setting  $\Theta = 0$  and  $k = 1$ . A radiatively black surface condition is represented by setting the  $\rho_0$  factor to zero. The RPV model is designed such that the amplitude of the BRF appears as a factor in a product of an angular function. This angular function, namely  $\check{\rho}_{\text{sfc}}(z_0, \mathbf{\Omega}_0, \mathbf{\Omega}; \Theta, k)$ , can be itself expanded in a Fourier series limited to the first two terms

$$\check{\rho}_{\text{sfc}}(z_0, \mu_0, -\mu, \phi_0 - \phi; \Theta, k) = r_0(\mu_0, -\mu; \Theta, k) + r_1(\mu_0, -\mu; \Theta, k) \cos(\phi_0 - \phi), \quad (14)$$

where the Fourier components,  $r_0(\mu_0, -\mu; \Theta, k)$  and  $r_1(\mu_0, -\mu; \Theta, k)$ , are defined using a formalism similar to that exploited earlier for the diffuse atmospheric transmission functions (6) and (7). These components satisfy the reciprocity principle. Assuming that such a principle holds for land surfaces certainly simplifies the design and exploitation of inverse algorithms (Martonchik et al. 1998b) but it is important to keep in mind that its validity is not universal and is somewhat resolution dependent. In particular, it is not applicable to structurally heterogeneous surfaces (Pinty et al. 2002; Widlowski et al. 2004).

The angular shape of the DHR can be estimated by integrating (14) over all upward directions

$$\check{A}(z_0, \mu_0; \Theta, k) = \frac{1}{\pi} \int_0^{2\pi} \int_0^1 \check{\rho}_{\text{sfc}}(z_0, \mu_0, -\mu, \phi_0 - \phi; \Theta, k) \mu \, d\mu \, d\phi = 2 \int_0^1 r_0(\mu_0, -\mu; \Theta, k) \mu \, d\mu. \quad (15)$$

This DHR is an intrinsic property of the surface, which does not depend on the distribution of the downwelling atmospheric intensity field.

The contribution of BRF angular field to the bihemispherical reflectance  $\text{BHR}_{\text{iso}}$ , under perfectly isotropic downward illumination conditions is equal to

$$\alpha_0(z_0; \Theta, k) = 4 \int_0^1 \int_0^1 r_0(\mu', -\mu; \Theta, k) \mu' \, d\mu' \, \mu \, d\mu; \quad (16)$$

$I_{\text{ms}}^{\downarrow \text{diff}}$  is associated to the flux density  $E_{\text{ms}}^{\downarrow \text{diff}}$ , such that  $I_{\text{ms}}^{\downarrow \text{diff}} = E_{\text{ms}}^{\downarrow \text{diff}}/\pi$  and earlier studies [see, for instance, Chandrasekhar (1960), Eq. (200) and Liou (1980), Eq. (6.181)] have shown that  $E_{\text{ms}}^{\downarrow \text{diff}}$  can be estimated with the following generic formula in the case of a radiatively isotropic surface

$$E_{\text{ms}}^{\downarrow \text{diff}}(z_0, \mu_0; \tau, \rho_{\text{sfc}}) \approx \frac{\psi[z_0; \rho_0 \alpha_0(z_0; \Theta, k), S(\tau)]}{1 - \psi[z_0; \rho_0 \alpha_0(z_0; \Theta, k), S(\tau)]} \times [E^{\downarrow \text{dir}}(z_0, \mu_0; \tau) + E_B^{\downarrow \text{diff}}(z_0, \mu_0; \tau)], \quad (17)$$

where the function  $\psi$  represents the source terms reaching the surface because of the multiple surface-atmosphere scattering interactions and  $S(\tau)$  is the so-called spherical albedo of the bottom of the atmosphere given by

$$S(\tau) = \frac{1}{\pi^2} \int_0^{2\pi} \int_0^1 \int_0^{2\pi} \int_0^1 \rho_{\text{atm}}(z_{\text{boa}}, -\mu, \mu', \phi' - \phi; \tau) \mu \, d\mu \, d\phi \, \mu' \, d\mu' \, d\phi'. \quad (18)$$

Although accurate enough for a large number of situations, this generic formulation for  $E_{\text{ms}}^{\downarrow \text{diff}}$  was shown to be in relative error by as much as 10% against accurate radiation transfer models, especially for overhead sun and under conditions where a significantly anisotropic bright surface is coupled with large atmospheric optical depth values (Lyapustin and Knyazikhin 2001). Indeed, (17) is written assuming that the directionality of the intensity fields scattered by the atmosphere and the surface is lost even from the very first interaction. This assumption overestimates or underestimates the contribution depending on the overall shape of the BRF: a bowl-shape (bell shape) BRF will induce an overestimation (underestimation). This is because the  $\alpha_0$  value intervening in the function  $\psi$  in the numerator of (17) is equal to the angular average over all  $\mu_0$  of the  $\check{A}$  function describing the shape of the DHR. Thus, for overhead sun, the first source term due to the surface must be systematically overestimated (underestimated) for bowl-shape (bell shape) BRF conditions.

Bowl-shape BRF conditions, the most common case at low spatial resolutions where various surface types are contributing to the radiation field, induce an increase of the DHR values with the sun zenith angle, a situation opposite to the one obtained for bell-shape BRF conditions that can be observed, for instance, when snow is covering the ground of boreal coniferous forest (Pinty et al. 2002). It is, however, easy to preserve some directionality in the function  $\psi$  and, in particular, the one induced by the first order of scattering by the surface. We can, indeed, define the functions  $\psi_1[z_0; \rho_0 \check{A}(z_0, \mu_0), S(\tau)]$ , which approximate the first source term scattered back to the atmosphere, and  $\psi_2[z_0; \rho_0 \alpha_0(z_0), S(\tau)]$ , which assumes that any scattering event involving the atmosphere, following a scattering event by the surface, introduces a loss of directionality, yielding a slight modification of (17):

$$E_{\text{ms}}^{\downarrow\text{diff}}(z_0, \mu_0; \tau, \rho_{\text{sfc}}) \approx \frac{\psi_1[z_0; \rho_0 \check{A}(z_0, \mu_0; \Theta, k), S(\tau)]}{1 - \psi_2[z_0; \rho_0 \alpha_0(z_0; \Theta, k), S(\tau)]} \times [E^{\downarrow\text{dir}}(z_0, \mu_0; \tau) + E_B^{\downarrow\text{diff}}(z_0, \mu_0; \tau)]. \quad (19)$$

Many more options could be considered in order to increase further the accuracy when estimating  $E_{\text{ms}}^{\downarrow\text{diff}}$ . The function  $\psi_1[z_0; \rho_0 \check{A}(z_0, \mu_0; \Theta, k), S(\tau)]$  could, for instance, also incorporate the directional hemispherical reflectance of the atmosphere instead of its spherical albedo.

According to (4) and (19), we thus obtain the following expression to approximate  $T_{\text{ms}}$ :

$$T_{\text{ms}}(z_0, \mu_0; \tau, \rho_{\text{sfc}}) \approx \frac{\check{A}(z_0, \mu_0; \Theta, k) S(\tau)}{1 - \rho_0 \alpha_0(z_0; \Theta, k) S(\tau)} \rho_0 \times \frac{[\exp(-\tau/\mu_0) + \bar{T}(\mu_0; \tau)]}{\pi}. \quad (20)$$

Since the three contributions for the downward intensity field as decomposed in (1) are now parameterized, the corresponding upward intensity field,  $I^{\uparrow\text{tot}}$ , can be expressed in any direction of interest  $\Omega(-\mu, \phi)$  as follows:

$$I^{\uparrow\text{tot}}(z_0, \mu_0, -\mu, \phi_0 - \phi; \tau, \rho_{\text{sfc}}) = \frac{\rho_0}{\pi} \int_0^{2\pi} \int_0^1 I^{\downarrow\text{tot}}(z_0, \mu_0, \mu', \phi_0 - \phi'; \tau, \rho_{\text{sfc}}) \times \check{\rho}_{\text{sfc}}(z_0, \mu', -\mu, \phi' - \phi; \Theta, k) \mu' d\mu' d\phi' = \frac{E_0 \mu_0}{\pi} \rho_0 \check{\rho}_{\text{sfc}}^H(z_0, \mu_0, -\mu, \phi_0 - \phi; \tau, \rho_{\text{sfc}}), \quad (21)$$

where  $\check{\rho}_{\text{sfc}}^H$  denotes the angular function of the surface bidirectional reflectance factor with respect to the total downwelling intensity field, including all sources scattered in the upward hemisphere. This angular function can further be approximated by

$$\check{\rho}_{\text{sfc}}^H(z_0, \mu_0, -\mu, \phi_0 - \phi; \tau, \rho_{\text{sfc}}) = \exp(-\tau/\mu_0) \check{\rho}_{\text{sfc}}(z_0, \mu_0, -\mu, \phi_0 - \phi; \Theta, k) + [f_0(\mu_0, -\mu; \tau, \Theta, k) + f_1(\mu_0, -\mu; \tau, \Theta, k) \cos(\phi_0 - \phi)] + \pi T_{\text{ms}}(z_0, \mu_0; \tau, \rho_{\text{sfc}}) \check{A}(z_0, -\mu; \Theta, k), \quad (22)$$

where

$$f_0(\mu_0, -\mu; \tau, \Theta, k) = 2\pi \int_0^1 T_0(\mu_0, \mu'; \tau) r_0(\mu', -\mu; \Theta, k) \mu' d\mu',$$

$$f_1(\mu_0, -\mu; \tau, \Theta, k) = \pi \int_0^1 T_1(\mu_0, \mu'; \tau) r_1(\mu', -\mu; \Theta, k) \mu' d\mu'. \quad (23)$$

These mathematical developments should permit us to represent accurately enough the coupling between the downwelling direct and diffuse atmospheric intensities and the anisotropic surface properties. This decomposition reaches a high relative accuracy (generally less than 2% of the intensities escaping at the top of the atmosphere) as compared to results delivered by high accuracy radiation transfer models (Martonchik et al. 2002; Pinty et al. 2000a). The absolute accuracy of the results depends on the performance of the radiation transfer models used to generate the original  $T_B, \check{\rho}_{\text{sfc}}$  functions as well as other functions and parameters associated with them.

### 3. From upward intensity fields to surface albedos

As stated earlier, the useful quantities needed by atmospheric global/regional models to deal with land surface processes include the surface albedo, in order to assess the flux absorbed in the media below the horizontal plane of reference, the level  $z_0$ , chosen to define the albedo. Usually, this ratio is then weighted as a function of the fraction of downward direct to diffuse density fluxes (see, e.g., Roesch et al. 2004). Following this, the albedo with respect to the total downward flux density is equivalent to a BHR thus estimated by

$$\text{BHR}(z_0, \mu_0; \tau, \rho_{\text{sfc}}) = \frac{E^{\uparrow\text{tot}}(z_0, \mu_0; \tau, \rho_{\text{sfc}})}{E^{\downarrow\text{tot}}(z_0, \mu_0; \tau, \rho_{\text{sfc}})}, \quad (24)$$

with

$$E^{\uparrow\text{tot}}(z_0, \mu_0; \tau, \rho_{\text{sfc}}) = \int_0^{2\pi} \int_0^1 I^{\uparrow\text{tot}}(z_0, \mu_0, -\mu, \phi - \phi_0; \tau, \rho_{\text{sfc}}) \mu d\mu d\phi \quad (25)$$

and

$$E^{\downarrow\text{tot}}(z_0, \mu_0; \tau, \rho_{\text{sfc}}) = \int_0^{2\pi} \int_0^1 I^{\downarrow\text{tot}}(z_0, \mu_0, \mu, \phi - \phi_0; \tau, \rho_{\text{sfc}}) \mu d\mu d\phi. \quad (26)$$

According to the notations and approximations introduced in section 2, the total downward flux density is equal to

$$E^{\downarrow\text{tot}}(z_0, \mu_0; \tau, \rho_{\text{sfc}}) = E_0 \mu_0 [\exp(-\tau/\mu_0) + \bar{T}(\mu_0; \tau) + \pi T_{\text{ms}}(z_0, \mu_0; \tau, \rho_{\text{sfc}})], \quad (27)$$

where  $\bar{T}(\mu_0; \tau)$  and  $T_{\text{ms}}(z_0, \mu_0; \tau, \rho_{\text{sfc}})$  are given by (12) and (20), respectively. The total upward flux density resulting from (25) is obtained as follows:

$$\begin{aligned} E^{\uparrow\text{tot}}(z_0, \mu_0; \tau, \rho_{\text{sfc}}) &= \frac{E_0 \mu_0}{\pi} \rho_0 \int_0^{2\pi} \int_0^1 \check{\rho}_{\text{sfc}}^H(z_0, \mu_0, -\mu, \phi_0 - \phi; \tau, \rho_{\text{sfc}}) \mu \, d\mu \, d\phi \\ &= E_0 \mu_0 \rho_0 [\exp(-\tau/\mu_0) \check{A}(z_0, \mu_0; \Theta, k) + \bar{f}_0(\mu_0; \tau, \Theta, k) + \pi T_{\text{ms}}(z_0, \mu_0; \tau, \rho_{\text{sfc}}) \alpha_0(z_0; \Theta, k)] \end{aligned} \quad (28)$$

and

$$\bar{f}_0(\mu_0; \tau, \Theta, k) = 2 \int_0^1 f_0(\mu_0, -\mu; \tau, \Theta, k) \mu \, d\mu, \quad (29)$$

yielding the following equation for the surface albedo:

$$\text{BHR}(z_0, \mu_0; \tau, \rho_{\text{sfc}}) = \rho_0 \times \frac{[\exp(-\tau/\mu_0) \check{A}(z_0, \mu_0; \Theta, k) + \bar{f}_0(\mu_0; \tau, \Theta, k) + \pi T_{\text{ms}}(z_0, \mu_0; \tau, \rho_{\text{sfc}}) \alpha_0(z_0; \Theta, k)]}{[\exp(-\tau/\mu_0) + \bar{T}(\mu_0; \tau) + \pi T_{\text{ms}}(z_0, \mu_0; \tau, \rho_{\text{sfc}})]}. \quad (30)$$

The mathematical developments and approximations proposed above are easy to implement as computationally efficient algorithms to estimate the surface albedo of an anisotropic surface illuminated by an anisotropic atmospheric diffuse intensity field. Indeed, all angular quantities, including those intervening in the various integrals can be precomputed and stored in lookup tables for a series of preselected atmospheric conditions characterized by a vertical optical thickness  $\tau$  and surface anisotropic conditions such as the  $\Theta$  and  $k$  parameters of the RPV model.

Factoring out the amplitude  $\rho_0$  of the surface BRF, which is the main contributor to the BHR/albedo values, renders (30) appealing for direct modeling pur-

poses. Indeed, simulations can be conducted over the range of sun angles deemed acceptable for a plane-parallel approach and over a very substantial part of the domain of variability of the state variables of the problem. As mentioned above, large datasets of the RPV model parameters (or their equivalent such as the MODIS kernels) are now available from various space agencies so that the probability distribution functions of these parameters controlling the angular field of the surface BRF are available at various wavelengths and spatial resolutions and over the entire range of surface conditions that can be encountered on earth.

Given that  $\rho_0 \check{A} \equiv \text{DHR}$  and  $\rho_0 \alpha_0 \equiv \text{BHR}_{\text{iso}}$ , respectively, (30) reduces to

$$\text{BHR}(z_0, \mu_0; \tau, \rho_{\text{sfc}}) = \text{DHR}(z_0, \mu_0; \rho_{\text{sfc}}) f^{\downarrow\text{dir}}(z_0, \mu_0; \tau) + \frac{\rho_0 \bar{f}_0(\mu_0; \tau, \Theta, k) + \pi T_{\text{ms}}(z_0, \mu_0; \tau, \rho_{\text{sfc}}) \text{BHR}_{\text{iso}}(z_0; \rho_{\text{sfc}})}{t^{\downarrow\text{tot}}(z_0, \mu_0; \tau, \rho_{\text{sfc}})}, \quad (31)$$

where  $t^{\downarrow\text{tot}}(z_0, \mu_0; \tau, \rho_{\text{sfc}})$  is the directional hemispherical transmission factor corresponding to the total downward flux density  $E^{\downarrow\text{tot}}$ ,  $f^{\downarrow\text{dir}}(z_0, \mu_0; \tau)$  is the ratio of direct to total flux density, that is,  $\exp(-\tau/\mu_0)/t^{\downarrow\text{tot}}$  and

$\text{BHR}_{\text{iso}}$  are the bihemispherical reflectance of the surface when illuminated by a perfectly isotropic intensity field. This latter contribution is introduced by the parameterization we adopted for representing the effects

due to multiple scattering between the surface and the atmosphere.

Equations (30) and (31) illustrate that, unlike the DHR, surface albedo is not an intrinsic characteristic of the land surfaces but is controlled by ambient atmospheric conditions. The values of surface albedo required by atmospheric models to accurately take into account surface-atmosphere interactions thus vary from place to place and from time to time, not only because of changes at the surface but also as a function of the spatial distributions of aerosols and clouds, for instance, as they greatly affect the anisotropy of the downwelling irradiance. However, both (30) and (31) suggest a simple and computer efficient scheme to ingest the appropriate information available from satellites and to properly account for these atmospheric effects.

Equation (31) is strictly equivalent to (30): both equations express surface albedo as a function of parameters and products that can be derived from space sensors exhibiting quasi-simultaneous multiangle capabilities, such as MISR (Diner et al. 1998) and to a lesser extent all geostationary satellites (Pinty et al. 2000a) or even single-angle sensors such as MODIS (SchAAF et al. 2002). In the case of MISR, for instance, the parameter values controlling the amplitude and shape of the surface BRDF are delivered together with the DHR values and a substantial characterization of the atmospheric conditions prevailing at the time of data acquisition (available online at <http://eosweb.larc.nasa.gov/>). Given that information, (31) provides a simple and physically coherent scheme to estimate surface albedo for sun zenith angle values other than the one at the time of the measurements.

The BHR estimated under ambient atmospheric conditions prevailing during the observing conditions is not extremely relevant for atmospheric modeling purposes. Indeed, surface albedo must be simulated under the atmospheric conditions generated by the atmospheric model itself. Adopting the technically practical assumption that the downward diffuse intensity field reaching the surface is perfectly isotropic, that is, independent of any direction  $\Omega(\mu, \phi)$ , (31) can be rewritten as follows [see, e.g., Kondratyev (1972), chapter 2; Lewis and Barnsley (1994)]:

$$\begin{aligned} \text{BHR}^*(z_0, \mu_0; \tau, \rho_{\text{sfc}}) &= \text{DHR}(z_0, \mu_0; \rho_{\text{sfc}}) f^{\text{dir}}(z_0, \mu_0; \tau) \\ &+ \text{BHR}_{\text{iso}}(z_0; \rho_{\text{sfc}}) f^{\text{diff}}(z_0, \mu_0; \tau, \rho_{\text{sfc}}), \end{aligned} \quad (32)$$

where  $f^{\text{diff}}(z_0, \mu_0; \tau, \rho_{\text{sfc}})$  denotes the fraction of diffuse to total downward flux density equal to

$$\begin{aligned} f^{\text{diff}}(z_0, \mu_0; \tau, \rho_{\text{sfc}}) &= 1 - f^{\text{dir}}(z_0, \mu_0; \tau) \\ &= \frac{\pi [T_{\text{iso}}(z_0, \mu_0; \tau) + T_{\text{ms}}(z_0, \mu_0; \tau, \rho_{\text{sfc}})]}{t^{\text{tot}}(z_0, \mu_0; \tau, \rho_{\text{sfc}})}, \end{aligned} \quad (33)$$

with

$$\begin{aligned} T_{\text{iso}}(z_0, \mu_0; \tau) &= \frac{1}{\pi} \int_0^{2\pi} \int_0^1 T_B(z_0, \mu_0, \mu, \phi_0 \\ &- \phi; \tau) \mu \, d\mu \, d\phi. \end{aligned} \quad (34)$$

Note also that  $T_{\text{iso}}(\mu_0; \tau) = \bar{T}(\mu_0; \tau)/\pi$  and  $\text{BHR}_{\text{iso}}(z_0; \rho_{\text{sfc}}) = \rho_0 \alpha_0(z_0; \Theta, k)$ . Given (34), the values of the hemispherical directional quantities  $f^{\text{diff}}$  and  $t^{\text{tot}}$  remain unchanged when assuming that the diffuse downwelling bidirectional transmission distribution function is isotropic.

As indicated by (32),  $\text{BHR}^*$  results from a simple weighting of two distinct surface albedo types, each associated with an extreme incident radiation field: the DHR, associated with an incident intensity field that is purely monodirectional and the  $\text{BHR}_{\text{iso}}$ , associated with an incident intensity field that is purely isotropic, and where the weights,  $f^{\text{dir}}$  and  $f^{\text{diff}}$ , sum up to 1. Following the MODIS terminology,  $\text{BHR}^*$  is named the blue sky albedo.

Figures 1 and 2 exhibit results of an intercomparison between the three types of surface albedo values considered here, namely  $\text{DHR}(z_0, \mu_0; \rho_{\text{sfc}})$ ,  $\text{BHR}(z_0, \mu_0; \tau, \rho_{\text{sfc}})$ , and  $\text{BHR}^*(z_0; \rho_{\text{sfc}})$ . The intercomparison is presented as a function of the sun zenith angle for the spectrally broadband visible (0.3–0.7  $\mu\text{m}$ ) and near-infrared (0.7–3.0  $\mu\text{m}$ ) regions of the solar spectrum, and for various aerosol optical thickness conditions. A relatively low (high) value of the surface albedo, prescribed through the  $\rho_0$  parameter of the RPV model, has been assigned to the visible (near infrared) in order to mimic the corresponding vegetated surface properties commonly observed over these spectral regions. On both figures, the top (bottom) panels show results obtained for a bowl-shape (bell shape) surface BRDF condition. In these simulations, the values chosen for the  $k$  parameter entering the RPV model (13) are equal to 0.6 (top panels) and 1.4 (bottom panels), respectively, in order to represent the bowl- versus bell-shape BRDF conditions (the  $\Theta$  parameter is set equal to 0.0 in all simulations so that there is no imbalance between forward and backward scattering). Note that such values for the  $k$  parameter are most likely to occur at high spatial resolution due to the natural mixing and merging of various surface types at medium spatial resolution (Pinty et al. 2002). The aerosol optical depth values at 0.5  $\mu\text{m}$  varies



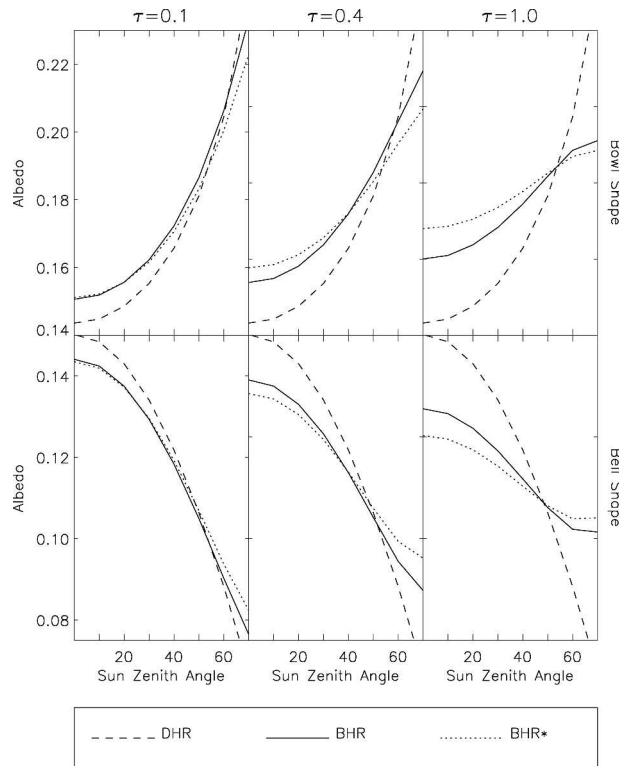


FIG. 1. Intercomparison of  $DHR(z_0, \mu_0; \rho_{sfc})$  (dashed line),  $BHR(z_0, \mu_0; \tau, \rho_{sfc})$  (solid line), and  $BHR^*(z_0, \mu_0; \tau, \rho_{sfc})$  (dotted line) values simulated for (top) bowl- and (bottom) bell-shaped surface BRF conditions as a function of the sun zenith angle for  $\rho_0$  equal 0.1. The aerosol optical depth values at  $0.5 \mu\text{m}$  vary between (left) 0.1, (middle) 0.4, and (right) 1.0. These simulations are performed in a broadband visible range, i.e., between  $0.3$  and  $0.7 \mu\text{m}$ , of the solar spectrum.

between 0.1 (left panels), 0.4 (middle panels), and 1.0 (right panels). The atmospheric functions have been calculated in the case of US-62 type of standard atmosphere implementing a continental aerosol model, which includes a mixture of dustlike, water-soluble, and soot components (see Vermote et al. 1997). The diffuse downwelling bidirectional transmission distribution function and all other aerosol-related functions are pre-computed using successive orders of scattering method.

For both bowl and bell surface BRF conditions, the smoothing effect due to atmospheric scattering is noticeable especially in the visible part of the spectrum and medium to high aerosol load. Indeed, for all surface and atmosphere conditions considered in these examples, the angular dependencies exhibited by the DHR values are always more pronounced than those observed for the two BHRs. With a bowl-shape (bell shape) surface BRF condition, the atmospheric scattering increases (reduces) the values estimated for close to nadir sun conditions. As expected, the effects induced

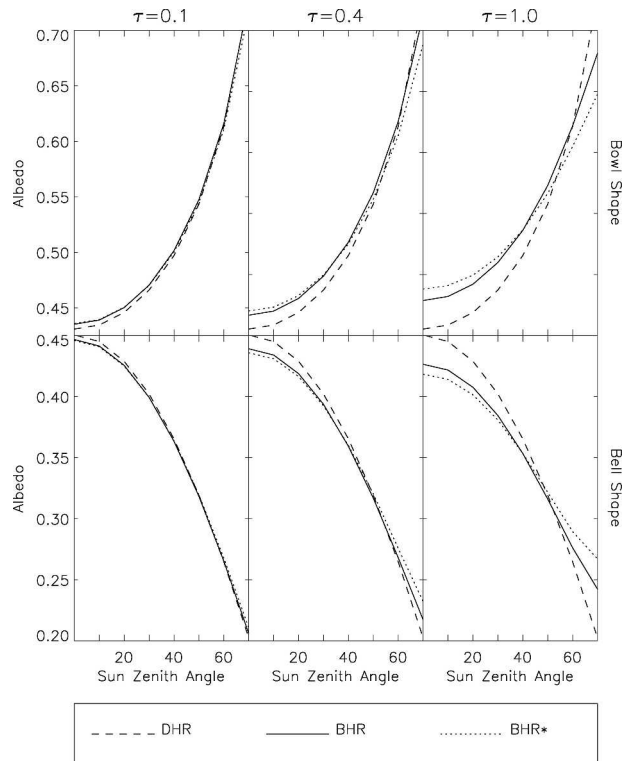


FIG. 2. Same as Fig. 1 except for the broadband near-infrared range ( $\rho_0 = 0.3$ ), i.e., between  $0.7$  and  $3.0 \mu\text{m}$ , of the solar spectrum.

by the atmospheric scattering contribution are weakened in the near-infrared region. For all studied conditions and in both spectral domains, the values of the BHR\* systematically underestimate the slope of the angular variation exhibited by the actual flux ratio, namely the BHR values. This is a direct consequence of accounting for the full atmosphere–surface coupling of the scattering processes. Such systematic biases induced by the atmospheric properties must be considered when conducting intercomparison exercises between various sources of surface albedo values (see, e.g., Jin et al. 2003; Roesch et al. 2004).

Although based on the more restrictive physical assumption of isotropic molecular and aerosol scattering typical of stratus cloud decks, (32) is attractive because it effectively offers a decoupling between the surface and the atmospheric scattering properties. The surface scattering properties are indeed specified through the DHR and the  $BHR_{iso}$  values, and any sort of atmospheric conditions can be addressed.

The difference introduced by assuming that the diffuse downwelling bidirectional transmission distribution function is isotropic can be assessed simply by comparing (31) and (32):

$$\begin{aligned} \Delta_{\text{BHR}}(z_0, \mu_0; \tau, \rho_{\text{sfc}}) &= \text{BHR}(z_0, \mu_0; \tau, \rho_{\text{sfc}}) \\ &\quad - \text{BHR}^*(z_0, \mu_0; \tau, \rho_{\text{sfc}}) \\ &= \rho_0 \zeta(z_0, \mu_0; \tau, \rho_{\text{sfc}}), \end{aligned} \quad (35)$$

with

$$\zeta(z_0, \mu_0; \tau, \rho_{\text{sfc}}) = \frac{[\bar{f}_0(\mu_0; \tau, \Theta, k) - \alpha_0(z_0; \Theta, k)\bar{T}(\mu_0; \tau)]}{t^{\downarrow \text{tot}}(z_0, \mu_0; \tau, \rho_{\text{sfc}})}. \quad (36)$$

Figure 3 illustrates, as a function of the sun zenith angle, the impact of the isotropic assumption based on estimates from (36) for a series of atmospheric and surface conditions. The top (bottom) panels exhibit results obtained for a bowl-shape (bell shape) surface BRF condition and the left (right) panels correspond to estimations over the visible (near infrared) region. For all practical purposes, the relative difference between both BHR values remain within bounds of  $\pm 10\%$ , as demonstrated by considering somewhat more extreme values that can be anticipated at medium spatial resolution for the RPV model  $k$  parameter under quite turbid aerosol optical depth conditions. As a matter of fact, the estimated trend and amplitude for  $\Delta_{\text{BHR}}$  falls within the range of those estimated by Lewis and Barnsley (1994), at least for the limited set of environmental conditions they considered. The need for properly describing the full surface-atmosphere coupling is thus dependent on the accuracy required by the application at hand. One must remember however that the bowl- or bell-shape anisotropy of the surface introduces systematic biases, as a function of the sun zenith angle, which are increasing with the aerosol load and the value of the  $k$  parameter value of the RPV surface BRF model.

Equation (32) can be applied straightforwardly using the DHR (called the black sky albedo) and associated  $\text{BHR}_{\text{iso}}$  (called the white sky albedo) products retrieved from data acquired by the MODIS instrument (available online at <http://edcdaac.usgs.gov/modis/dataproducts.asp>). For applications requiring an accuracy higher than is possible with (32), for instance, validation against field measurements (Jin et al. 2003), it is simple to account for the additional coupling contribution as expressed by the factor  $\Delta_{\text{BHR}}$ , that is,

$$\begin{aligned} \text{BHR}(z_0, \mu_0; \tau, \rho_{\text{sfc}}) &= \text{BHR}^*(z_0, \mu_0; \tau, \rho_{\text{sfc}}) \\ &\quad + \Delta_{\text{BHR}}(z_0, \mu_0; \tau, \rho_{\text{sfc}}). \end{aligned} \quad (37)$$

As explained previously, the parameters and functions intervening in (36) can be precomputed and stored in

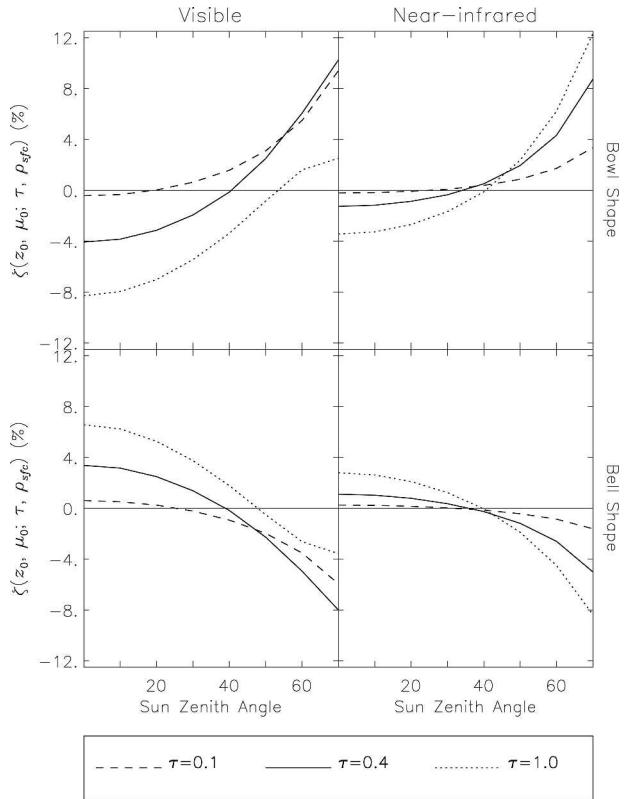


FIG. 3. Values of  $\zeta(z_0, \mu_0; \tau, \rho_{\text{sfc}})$  [see (36)] as a function of the sun zenith angle for a series of atmospheric and surface conditions (same as in Figs. 1 and 2). Results obtained for (top) bowl- and (bottom) bell-shaped surface BRF conditions, and estimations over the (left) broadband visible and (right) near-infrared spectral region. The aerosol optical depth values at  $0.5 \mu\text{m}$  vary between 0.1 (dashed line), 0.4 (solid line), and 1.0 (dotted line).

lookup tables. The surface related factors needed as input to estimate these quantities are directly available from the MISR instrument and can be, to some extent, estimated from products delivered by the MODIS instrument. The suite of products associated with the approach developed for the retrieval of surface albedo values from the series of Meteosat geostationary satellites (Pinty et al. 2000b) encloses all the surface and atmospheric parameters required by (30), (31), or (37).

#### 4. Conclusions

The proposed developments aim at documenting the various meanings of the expression surface albedo that was shown to correspond to a variety of physical quantities. Our analytical approach permits us 1) to contrast the various albedo products currently delivered by space agencies, as well as stressing their complementarity, 2) to establish a series of relationships linking the various types of albedo, and 3) to apply a simple

physically based approach to perform an accurate coupling between the surface and atmospheric scattering properties. In the process, analytical relationships are established to allow the estimation of the various types of albedo for any desired sun zenith angle conditions. Such relationships should prove useful to bridge the gap between the remote sensing derived products and the modeling needs of the atmospheric community.

The main albedo quantities considered here are the directional hemispherical reflectance, DHR (or equivalently the black sky albedo), the bihemispherical reflectance, BHR, and the bihemispherical reflectance under isotropic diffuse sky irradiance,  $BHR_{iso}$  (or equivalently the white sky albedo). These quantities all correspond to ratios between downward and upward fluxes and they basically differ only by the way the coupling between the surface and atmospheric scattering properties is handled. Simulation studies conducted to bound theoretical atmospheric and surface conditions illustrate, for instance, that if one depends on the type of albedo some small but systematic biases may be introduced as a function of the illumination angle. Although these simulations do not cover the most extreme conditions that can be encountered on earth, for example snow cover in forested area conditions, they do represent test cases probably more representative of higher spatial resolution sensors than those relevant for the MODIS, Meteosat, and MISR instruments. These simulations thus provide indications about the upper bounds of the angular trends and amplitude differences that may exist between the three commonly used albedo quantities. It was shown, for instance, that the assumption of an isotropic diffuse sky irradiance yields relative albedo errors/biases well within bounds of  $\pm 10\%$  and, therefore, close to uncertainty level expected for the remote sensing derived products. Such a range is therefore probably acceptable for a number of geophysical applications and only exceeds the accuracy required by many climate applications and surface albedo validation exercises when somewhat turbid conditions prevail.

The delivery of a suite of surface albedo products by space agencies is a very significant achievement and opens new research avenues for better understanding a range of land surface processes. Our developments also show that the auxiliary parameters describing the shape of the surface BRF are required for an accurate modeling of the radiant flux ratios, namely the BHRs, for any given solar position. Given this state of affairs regarding remote sensing product availability on the one hand, and the atmospheric models on the other hand, it appears that we now have access to very relevant information helpful for improving the representation of

the surface albedo as well as describing and accurately accounting for its spatial and temporal changes.

The construction of an approximate BHR from a computed or stored DHR and  $BHR_{iso}$  (isotropic diffuse fluxes assumed) is now within the capability of most climate models, that is, those whose computation of atmospheric solar radiation distinguishes between direct beam and diffuse beam radiation. Although the more advanced treatments of land include such a computation, they are only beginning to constrain their treatments to match the available new satellite data. Further inclusion of the directionality of diffuse radiation in computing land albedos as derived in this paper will require atmospheric models with solar radiation calculations including enough detail to provide the requisite directionality.

*Acknowledgments.* This research would not have been possible without the support of the Global Vegetation Monitoring unit of the Institute for Environment and Sustainability at the Joint Research Centre, an institution of the European Commission. This manuscript benefited from the careful reading and positive comments of Dr. Crystal B. Schaaf and an anonymous reviewer.

#### REFERENCES

- Chandrasekhar, S., 1960: *Radiative Transfer*. Dover, 393 pp.
- Diner, D. J., and Coauthors, 1998: Multi-angle Imaging Spectro-Radiometer MISR instrument description and overview. *IEEE Trans. Geosci. Remote Sens.*, **36**, 1072–1087.
- Heney, L. G., and T. L. Greenstein, 1941: Diffuse radiation in the galaxy. *Astrophys. J.*, **93**, 70–83.
- Jin, Y., C. B. Schaaf, C. E. Woodcock, F. Gao, X. Li, and A. H. Strahler, 2003: Consistency of MODIS surface bidirectional reflectance distribution function and albedo retrievals. 2. Validation. *J. Geophys. Res.*, **108**, D12105, doi:10.1029/2004JD004552.
- Knorr, W., K. G. Schnitzler, and Y. Govaerts, 2001: The role of bright desert regions in shaping North African climate. *Geophys. Res. Lett.*, **28**, 3489–3492.
- Kondratyev, K., 1972: *Radiation Processes in the Atmosphere*. World Meteorological Organization, 214 pp.
- Lenoble, J., 1985: *Radiative Transfer in Scattering and Absorbing Atmospheres: Standard Computational Procedures*. A. Deepak, 300 pp.
- Lewis, P., and M. Barnsley, 1994: Influence of the sky radiance distribution on various formulations of the earth surface albedo. *Proc. Sixth ISPRS Int. Symp. on Physical Measurements and Signatures in Remote Sensing*, Val d'Isère, France, Centre National D'études Spatiales, 707–715.
- Liou, K. N., 1980: *An Introduction on Atmospheric Radiation*. Academic Press, 392 pp.
- Lyapustin, A., 2002: Radiative transfer code SHARM-3D for radiance simulations over a non-Lambertian nonhomogeneous surface: Intercomparison study. *Appl. Opt.*, **41**, 5607–5615.

- , and Y. Knyazikhin, 2001: Green's function method for the radiative transfer problem. I: Homogeneous non-Lambertian surface. *Appl. Opt.*, **40**, 3495–3501.
- Martonchik, J. V., D. J. Diner, R. A. Kahn, T. P. Ackerman, M. M. Verstraete, B. Pinty, and H. R. Gordon, 1998a: Techniques for the retrieval of aerosol properties over land and ocean using multi-angle imaging. *IEEE Trans. Geosci. Remote Sens.*, **36**, 1212–1227.
- , —, B. Pinty, M. M. Verstraete, R. B. Myneni, Y. Knyazikhin, and H. R. Gordon, 1998b: Determination of land and ocean reflective, radiative, and biophysical properties using multiangle imaging. *IEEE Trans. Geosci. Remote Sens.*, **36**, 1266–1281.
- , C. J. Bruegge, and A. H. Strahler, 2000: A review of reflectance nomenclature for remote sensing. *Remote Sens. Rev.*, **19**, 9–20.
- , B. Pinty, and M. M. Verstraete, 2002: Note on an improved model of surface BRDF–atmospheric coupled radiation. *IEEE Trans. Geosci. Remote Sens.*, **40**, 1637–1639.
- Minnaert, M., 1941: The reciprocity principle in lunar photometry. *Astrophys. J.*, **93**, 403–410.
- Nicodemus, F. E., J. C. Richmond, J. J. Hsia, I. W. Ginsberg, and T. Limperis, 1977: *Geometrical Considerations and Nomenclature for Reflectance*. NBS Monogr., No. 160, National Bureau of Standards, U.S. Department of Commerce, 52 pp.
- Pinty, B., F. Roveda, M. M. Verstraete, N. Gobron, Y. Govaerts, J. Martonchik, D. Diner, and R. Kahn, 2000a: Surface albedo retrieval from METEOSAT. Part 1: Theory. *J. Geophys. Res.*, **105**, 18 099–18 112.
- , —, —, —, —, —, and —, 2000b: Surface albedo retrieval from METEOSAT. Part 2: Application. *J. Geophys. Res.*, **105**, 18 113–18 134.
- , J.-L. Widlowski, N. Gobron, M. M. Verstraete, and D. J. Diner, 2002: Uniqueness of multi-angular measurements. Part 1: A subpixel surface heterogeneity indicator from MISR. *IEEE Trans. Geosci. Remote Sens.*, **40**, 1560–1573.
- , and Coauthors, 2003: Earthquake-related dewatering using MISR/Terra satellite data. *Eos, Trans. Amer. Geophys. Union*, **84**, 37–48.
- Rahman, H., B. Pinty, and M. M. Verstraete, 1993: Coupled surface–atmosphere reflectance (CSAR) model. 2. Semiempirical surface model usable with NOAA Advanced Very High Resolution Radiometer data. *J. Geophys. Res.*, **98**, 20 791–20 801.
- Roesch, A., C. B. Schaaf, and F. Gao, 2004: Use of Moderate-Resolution Imaging Spectroradiometer bidirectional reflectance distribution function products to enhance simulated surface albedos. *J. Geophys. Res.*, **109**, D12105, doi:10.1029/2004JD004552.
- Schaaf, C. B., and Coauthors, 2002: First operational BRDF, albedo and nadir reflectance products from MODIS. *Remote Sens. Environ.*, **83**, 135–148.
- Vermote, E., D. Tanré, J. L. Deuzé, M. Herman, and J. J. Morcrette, 1997: Second simulation of the satellite signal in the solar spectrum: An overview. *IEEE Trans. Geosci. Remote Sens.*, **35**–3, 675–686.
- Verstraete, M. M., 1989: Land surface processes in climate models: Status and prospects. *Climate and the Geosciences: A Challenge for Science and Society in the 21st Century*, A. Berger, S. H. Schneider, and J. C. Duplessy, Eds., Kluwer Academic, 321–340.
- Widlowski, J.-L., B. Pinty, N. Gobron, M. M. Verstraete, D. J. Diner, and A. B. Davis, 2004: Canopy structure parameters derived from multi-angular remote sensing data for terrestrial carbon studies. *Climatic Change*, **65**, 403–415.
- Zhou, L., and Coauthors, 2003: Comparison of seasonal and spatial variations of albedos from moderate resolution imaging spectroradiometer (MODIS) and common land model. *J. Geophys. Res.*, **108**, 4488, doi:10.1029/2002JD003326.